J|A|C|S
ARTICLES

Published on Web 01/15/2009

Ultrafast Energy Transfer in Oligofluorene−Aluminum Bis(8-hydroxyquinoline)acetylacetone Coordination Polymers

Victor A. Montes, Grigory V. Zyryanov, Evgeny Danilov, Neeraj Agarwal, Manuel A. Palacios, and Pavel Anzenbacher, Jr.*

Department of Chemistry and Center for Photochemical Sciences, Bowling Green State University, Bowling Green, Ohio 43403

Received July 4, 2008; E-mail: pavel@bgsu.edu

Abstract: Understanding the excited-state dynamics in conjugated systems can lead to their better utilization in optical sensors, organic photovoltaics (OPVs), and organic light-emitting diodes (OLEDs). We present the synthesis of self-assembled coordination polymers comprising two types of fluorescent moieties: discrete fluorene oligomers of a well-defined length ($n = 1-9$) connected via aluminum(III) bis(8-quinolinolate)acetylacetone joints. Due to their well-defined structure, these materials allowed for a detailed study of energy migration processes within the materials. Thus, femtosecond transient spectroscopy was used to study the ultrafast energy transfer from the oligofluorene to the quinolinolate moieties, which was found to proceed at a rate of 10^{11} s^{-1}. The experimental results were found to be in agreement with the behavior predicted according to the Beljonne's improved Förster model of energy transfer. In addition, the solid-state and semiconductor properties of these coordination polymers allowed for the fabrication of OLEDs. Preliminary experiments with simple two- and three-layer devices fabricated by spin-coating yield bright yellow electroluminescence with maximum brightness of 6000 cd/m^2, with a turn-on voltage of ~6 V and a maximum external quantum efficiency of up to 1.2%, suggesting their potential for use in PLED applications.

Introduction

Excited-state resonance energy transfer[1] plays a pivotal role in numerous natural processes including the photosynthesis,[2] imaging, and diagnostics,[3] as well as in various applications such as (bio)chemical sensing,[4] photovoltaics,[5] and organic light-emitting devices (OLEDs).[6] In conjugated polymers,[7,8] energy transfer and exciton migration processes are very efficient and therefore can be exploited in amplifying sensors response,[9,10] exciton migration toward dissociation zones in solar cells,[11,12] and controlling the output of OLEDs.[13] Recently, the mechanisms of energy (exciton) migration in conjugated systems have been widely investigated in order to better understand their electronic properties,[14,15] which are of fundamental interest not only from an academic viewpoint but also because of their use in real-life applications.

(1) (a) May, V.; Kuhn, O. *Charge and Energy Transfer Dynamics in Molecular Systems*; Wiley-VCH: Berlin, 2000. (b) *Resonance Energy Transfer*; Andrews, D. L., Demidov, A. A., Eds.; Wiley: Chichester, 1999.
(2) (a) Gust, D.; Moore, T. A.; Moore, A. L. *Acc. Chem. Res.* **2001**, *34*, 40. (b) Wasielewski, M. R. *J. Org. Chem.* **2006**, *71*, 5051.
(3) *Biomedical Photonics Handbook*; Vo-Dinh, T., Ed.; CRC Press: Boca Raton, FL, 2003.
(4) Lakowicz, J. R. *Principles of Fluorescence Spectroscopy*; Springer: New York, 2006, p 458.
(5) Brédas, J.-L.; Beljonne, D.; Coropceanu, V.; Cornil, J. *Chem. Rev.* **2004**, *104*, 4971.
(6) (a) Bulovic, V.; Baldo, M. A.; Forrest, S. R. In *Organic Electronic Materials*; Farchioni, R., Grosso, G., Eds.; Springer: Berlin, 2001, p 391. (b) Baldo, M. A.; Forrest, S. R.; Thompson, M. E. In *Organic Electroluminescence*; Kafafi, Z. H., Ed.; Taylor and Francis: Boca Raton, FL, 2005, p 274.
(7) *Conjugated Polymers: Theory, Synthesis, Properties, and Characterization*; Skotheim, T. A., Reynolds, J., Eds.; CRC Press: Boca Raton, FL, 2007.
(8) Barford, W. *Electronic and Optical Properties of Conjugated Polymers*; Oxford University Press: Oxford, 2005.
(9) (a) McQuade, D. T.; Pullen, A. E.; Swager, T. M. *Chem. Rev.* **2000**, *100*, 2537. (b) Chen, L.; McBranch, D. W.; Wang, H.; Helgeson, R.; Wudl, F.; Whitten, D. G. *Proc. Natl. Acad. Sci. U.S.A.* **1999**, *96*, 12287. (c) Jones, R. L.; Lu, L.; Hegelson, R.; Bergstedt, T. S.; McBranch, D.; Whitten, D. G. *Proc. Natl. Acad. Sci. U.S.A.* **2001**, *98*, 14769. (d) Wang, D.; Gong, X.; Heeger, P. S.; Rininsland, F.; Bazan, G. C.; Heeger, A. J. *Proc. Natl. Acad. Sci. U.S.A.* **2002**, *99*, 49.
(10) (a) Zhou, Q.; Swager, T. M. *J. Am. Chem. Soc.* **1995**, *117*, 12593. (b) McQuade, D. T.; Hegedus, A. H.; Swager, T. M. *J. Am. Chem. Soc.* **2000**, *122*, 12389. (c) Stork, M.; Gaylord, B. S.; Heeger, A. J.; Bazan, G. C. *Adv. Mater.* **2002**, *14*, 361.
(11) *Organic Photovoltaics: Concepts and Realization*; Brabec, C., Dyakanov, V., Parisi, J., Sariciftci, N. S., Eds.; Springer: Berlin, 2003.
(12) (a) Halls, J. J.; Walsh, C. A.; Greenham, N. C.; Marseglia, E. A.; Friend, R. H.; Moratti, S. C.; Holmes, A. B. *Nature* **1995**, *376*, 498. (b) Sariciftci, N. S.; Smilowitz, L.; Heeger, A. J.; Wudl, F. *Science* **1992**, *258*, 1474. (c) Yu, G.; Gao, J.; Hummelen, J. C.; Wudl, F.; Heeger, A. J. *Science* **1995**, *270*, 1789.
(13) (a) Ego, C.; Marsitzky, D.; Becker, S.; Zhang, J.; Grimsdale, A. C.; Müllen, K.; MacKenzie, J. D.; Silva, C.; Friend, R. H. *J. Am. Chem. Soc.* **2003**, *125*, 437. (b) Wang, H.-L.; McBranch, D.; Klimov, V. I.; Helgerson, R.; Wudl, F. *Chem. Phys. Lett.* **1999**, *315*, 173.
(14) (a) Beljonne, D.; Pourtois, G.; Silva, C.; Hennebicq, E.; Herz, L. M.; Friend, R. H.; Scholes, G. D.; Setayeshi, S.; Müllen, K.; Brédas, J. L. *Proc. Natl. Acad. Sci. U.S.A.* **2002**, *99*, 10982. (b) Hennebicq, E.; Pourtois, G.; Scholes, G. D.; Herz, L. M.; Russell, D. M.; Silva, C.; Setayesh, S.; Grimsdale, A. C.; Müllen, K.; Brédas, J. L.; Beljonne, D. *J. Am. Chem. Soc.* **2005**, *127*, 4744. (c) Becker, K.; Lupton, J. M.; Feldmann, J.; Setayesh, S.; Grimsdale, A. C.; Müllen, K. *J. Am. Chem. Soc.* **2006**, *128*, 680. (d) Becker, K.; Lupton, J. M. *J. Am. Chem. Soc.* **2006**, *128*, 6468.
(15) (a) Tan, C.; Atas, E.; Muller, J. G.; Pinto, M. R.; Kleiman, V. D.; Schanze, K. S. *J. Am. Chem. Soc.* **2004**, *126*, 13685. (b) Nesterov, E. E.; Zhu, Z.; Swager, T. M. *J. Am. Chem. Soc.* **2005**, *127*, 10083.

Chart 1. Chemical Structure of Coordination Polymers **1a**−**e**

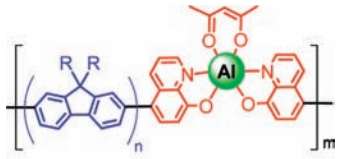

1

In general, the theoretical analysis of energy migration in conjugated polymers requires advanced models to account for the significant exciton delocalization and to estimate the electronic coupling between neighboring fragments.[16,17] One of the examples was reported by Beljonne et. al who developed an improved Förster formalism to describe the energy transfer between polyindenofluorene and perylene dye endcaps.[14b] In this work, exciton hopping rates were estimated and the transient photoluminescence was simulated qualitatively to describe the energy transfer process. However, strict predictions of the exciton dynamics in conjugated polymers are very complicated due to the irregular distribution of energy donor (D) and acceptor (A) sites arising from partial loss of electronic coupling due to statistic nature of the conformational processes, as well as potential traps resulting from structural defects introduced during their preparation. The structural inhomogeneities in conjugated polymers such as chain defects or kinks are difficult to detect by analytical techniques, but may still substantially limit the electronic communication taking place in the polymer.[18]

Conjugated materials with well-defined donor−acceptor (D−A) distances studied by Meijer et al.[19] are of significant advantage for studies of energy migration in hydrogen-bonded supramolecular structures of different sizes that combine the electronic properties of well-defined oligomers with the processability of polymeric structures.[19,20] However, energy transfer in these hydrogen-bonded systems has been studied only by steady-state methods lacking the time-resolved characterization.[19] To provide a detailed insight into the energy migration mechanism in conjugated systems and the time scale of exciton migration in self-assembled structures that combine donor and acceptor moieties at well-defined distances, fluorene oligomers (n = 1−9) connected via aluminum(III) bis(8-quinolinolate) acetylacetone complexes were synthesized (see Chart 1). The evolution of the energy transfer rate with an increasing oligofluorene length was compared to the prediction of the model put forward by Beljonne, and experimental evidence to support the theoretical treatment of singlet exciton migration in rigidly linked conjugated systems is provided. Compared to the energy transfer in solution, the solid-state studies revealed slightly different properties to the solution behavior. This insight was used in the preparation of simple OLEDs. Overall, the present results highlight the potential of self-assembled conjugated-coordination polymers as models for energy transfer studies, as well as a new class of functional conjugated materials.

Results and Discussion

Synthesis. A limited number of coordination polymers[21] were demonstrated to display electroluminescence. These were self-assembled polymers in which the zinc atoms have been used to template the assembly of organic ligands into coordination polymers.[22,23]

We decided to utilize an 8-hydroxyquinoline (HQ, oxinate)−Al^{III} mediated self-assembly synthetic approach for the construction of well-defined bichromophoric systems **1a**−**e**. In order to avoid the formation of dendritic structures around the octahedral geometry of the aluminum center, a 2,4-pentanedionate (acetylacetonate, acac) ancillary ligand was introduced. Moreover, the presence of acac ligands in the coordination sphere of aluminum quinolinolates has been reported to be beneficial for the electroluminescence performance of Alq_3.[24]

We found that two acetylacetonate ligands can be selectively replaced from $Al(acac)_3$ by 8-hydroxyquinoline under mild conditions to afford the heteroleptic complex, bis(8-quinolinolate)(acetylacetonate)aluminum(III), $Alq_2(acac)$, in high yield (see Scheme 1). We presumed that reaction of $Al(acac)_3$ with ditopic ligands of the general structure HQ-(fluorene)$_n$-HQ would afford polymeric materials driven by coordination to aluminum centers. Thus, the coordination polymers **1a**−**e** were prepared by self-assembly of the HQ-(fluorene)$_n$-HQ ditopic ligands in the presence of $Al(acac)_3$ in toluene (see the Supporting Information for synthetic details). The polymers were characterized by ^{1}H NMR and GPC analysis, which confirmed the polymeric nature of the materials (M_n = 6.1−42.1 kDa, 12 repeating units on average). As expected, the coordination polymers **1a**−**e** were soluble in a range of common organic solvents such as dichloromethane, toluene, chloroform, and tetrahydrofuran.

The ditopic ligands utilized for the synthesis of coordination polymers **1a**−**e** were synthesized according to the published procedure[25] using selective desymmetrization of the oligofluorene structure by monolithiation to introduce the trimethylsilyl (TMS) protecting group,[26] iodo-desilylation by ICl ipso-substitution of the protecting TMS group,[26,27] palladium-catalyzed preparation of fluorene boronic acid esters,[28] palladium-catalyzed cross-couplings,[29] and deprotection of the benzyl

(16) (a) Spano, F. C.; Meskers, S. C. J.; Hennebicq, E.; Beljonne, D. *J. Am. Chem. Soc.* **2007**, *129*, 7044. (b) Beljonne, D.; Hennebicq, E.; Daniel, C.; Herz, L. M.; Silva, C.; Scholes, G. D.; Hoeben, F. J. M.; Jonkheijm, P.; Schenning, A. P. H. J.; Meskers, S. C. J.; Phillips, R. T.; Friend, R. H.; Meijer, E. W *J. Phys. Chem. B* **2005**, *109*, 10594.
(17) (a) Van Averbeke, B.; Beljonne, D.; Hennebicq, E. *Adv. Funct. Mater.* **2008**, *18*, 492. (b) Bacchiocchi, C.; Hennebicq, E.; Orlandi, S.; Muccioli, L.; Beljonne, D.; Zannoni, C. *J. Phys. Chem. B* **2008**, *112*, 1752.
(18) Hennebicq, E.; Deleener, C.; Bredas, J.-L.; Scholes, G. D.; Beljonne, D. *J. Chem. Phys.* **2006**, *125*, 054901.
(19) Dudek, S. P.; Pouderoijen, M.; Abbel, R.; Schenning, A. P. H. J.; Meijer, E. W. *J. Am. Chem. Soc.* **2005**, *127*, 11763.
(20) El-ghayoury, A.; Schenning, A. P. H. J.; van Hal, P. A.; van Duren, J. K. J.; Janssen, R. A. J.; Meijer, E. W. *Angew. Chem., Int. Ed.* **2001**, *40*, 3660.
(21) (a) Archer, R. D. *Inorganic and Organometallic Polymers*; Wiley-VCH: New York, 2001. (b) Chandrasekhar, V. *Inorganic and Organometallic Polymers*; Springer: New York, 2005.
(22) (a) Yu, S.-C.; Kwok, C.-C.; Chan, W.-K.; Che, C.-M. *Adv. Mater.* **2003**, *15*, 1643. (b) Kwok, C.-C.; Yu, S.-C.; Sham, I. H. T.; Che, C.-M. *Chem. Commun.* **2004**, 2758.
(23) (a) Papadimitrakopoulos, F.; Thomsen, D. L., III.; Higginson, K. A. *Mater. Res. Soc. Symp. Proc.* **1998**, *488*, 105. (b) Papadimitrakopoulos, F.; Thomsen, D. L., III; Higginson, K. A. *Proc. SPIE* **1997**, *3148*, 170. (c) Thomsen, D. L., III; Phely-Bobin, T.; Papadimitrakopoulos, F. *J. Am. Chem. Soc.* **1998**, *120*, 6177.
(24) Xu, B.; Chen, L.; Liu, X.; Zhou, H.; Xu, H.; Fang, X.; Wang, Y. *Appl. Phys. Lett.* **2008**, *92*, 103305.
(25) Palacios, M. A.; Wang, Z.; Montes, V. A.; Zyryanov, G.; Hausch, B.; Jursíková, K.; Anzenbacher, P., Jr. *Chem. Commun.* **2007**, 3708.
(26) Li, B.; Li, Y.; Yaqin, F.; Bo, Z. *J. Am. Chem. Soc.* **2004**, *126*, 3430.
(27) Geng, Y.; Trajkovska, A.; Katsis, D.; Ou, J. J.; Culligan, S. W.; Chen, S. H. *J. Am. Chem. Soc.* **2002**, *124*, 8337.
(28) (a) Negishi, E. *Handbook of organopalladium chemistry for organic synthesis*, 5th ed.; de Meijere, A., Ed.; Wiley-Interscience: New York, 2002; Vol. 1. (b) Jo, J.; Chi, C.; Hoeger, S.; Wegner, G.; Yoon, D. Y. *Chem.−Eur. J.* **2004**, *10*, 2681.

Scheme 1. Synthesis of $Alq_2(acac)$ and Coordination Polymers **1a**−**e** Using Tris(acetylacetonate)aluminum(III), and X-ray Structure of $Alq_2(acac)$[a]

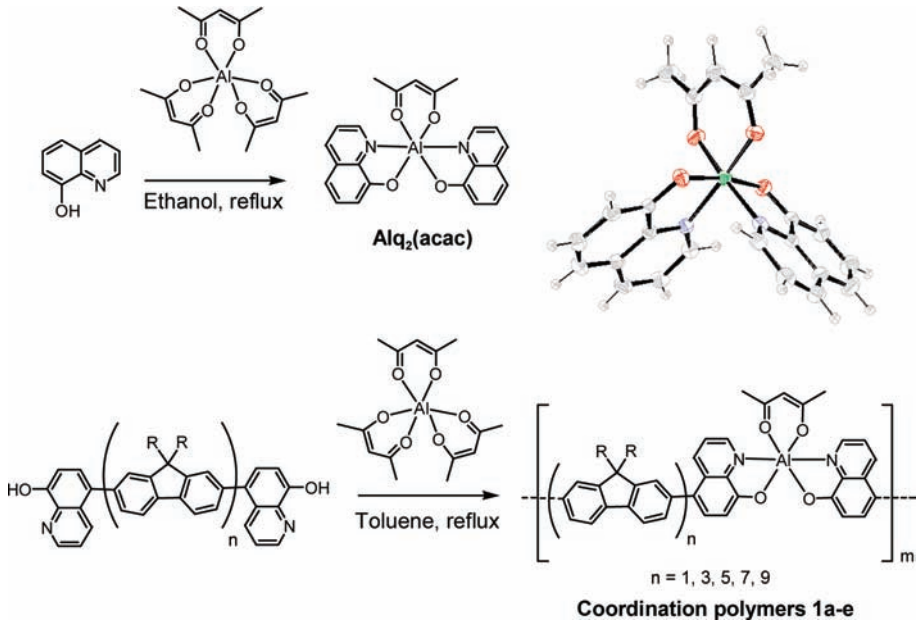

[a] The thermal ellipsoids were scaled to the 50% probability level.

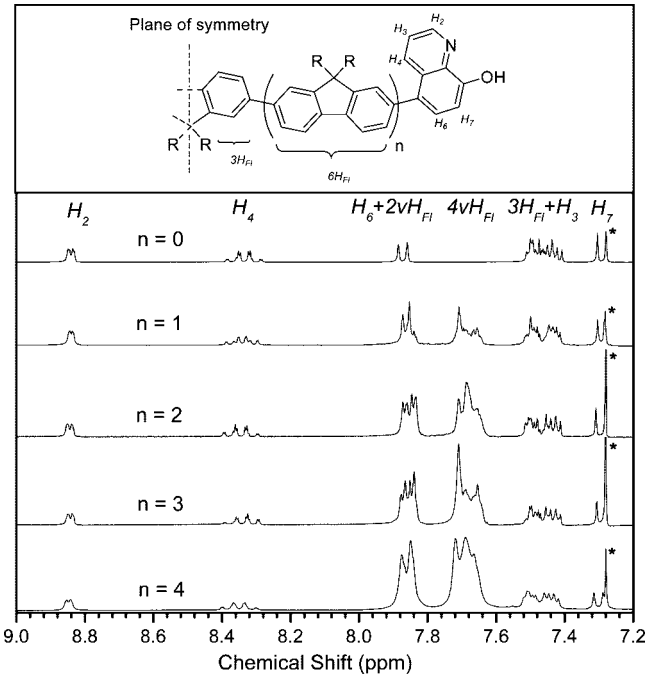

Figure 1. ^{1}H NMR spectra of the ditopic ligands. The increase of signals from fluorene moieties is clearly observed in the spectra,[27] with the general formula and proton assignment describing the proton distribution. The well-resolved resonances of quinoline at δ = 8.85 (H2), 8.35 (H4), and 7.29 ppm (H7) were observed. Residual $CHCl_3$ signals are marked with an asterisk.

group by transfer hydrogenation.[30] Figure 1 shows the assignment of the aromatic signals in ^{1}H NMR spectra of the synthesized building blocks.

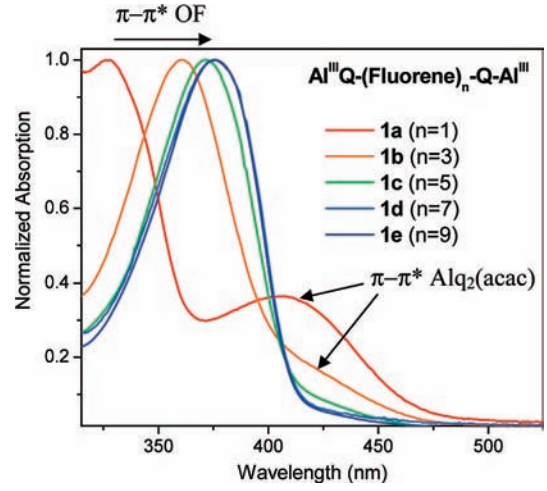

Figure 2. UV−vis absorption spectra of **1a**−**e** in a CH_2Cl_2 solution showing contribution of both oligofluorene (OF) and Al^{III} quinolinolate chromophores.

Optical Properties of the Bichromophoric Coordination Polymers. The formation of the coordination polymers results in establishing two distinctly different chromophores: the conjugated arylene backbone and the $Alq_2(acac)$ complex, both showing distinct spectroscopic behavior. The UV−visible absorption spectra of the coordination polymers **1a**−**e** were recorded at room temperature in CH_2Cl_2 and are shown in Figure 2. The spectra showed contributions of both the aluminum quinolinolate and oligofluorene (OF) chromophores, with the former becoming less prominent as the oligofluorene absorption increased with length.

Interestingly, the UV−visible spectra of **1a**−**e** also showed behavior typical for extended conjugated species. Specifically, the $\pi-\pi^*$ absorption band corresponding to the aluminum quinolinolate moiety (λ_{max} = 388 nm, 3.20 eV)[31] is shifted to lower energy for **1a**−**e** (405 nm, 3.06 eV), indicating extended conjugation in these ligands. Similarly, the absorption bands

(29) (a) Miyaura, N.; Suzuki, A. *Chem. Rev.* **1995**, *95*, 2457. (b) Bell, T. D. M.; Jacob, J.; Angeles-Izquierdo, M.; Fron, E.; Nolde, F.; Hofkens, J.; Müllen, K.; De Schryver, F. C. *Chem. Commun.* **2005**, 4973.
(30) Nakano, Y.; Imai, D. *Synthesis* **1997**, 1425.

Table 1. Summarized Absorption Data for Bichromophoric Systems **1a**−**e**

system	*n* (fluorene units)	λ_{max} [ε (M^{-1} cm^{-1})]	ΔE (eV)[a]
1a	1	327 [6.4×10^4], 405 [2.2×10^4]	0.19
1b	3	362 [9.1×10^4]	0.11
1c	5	372 [1.3×10^5]	0.07
1d	7	375 [4.1×10^5]	0.02
1e	9	376 [5.1×10^5]	0.00

[a] Difference in energy for the $S_0 \rightarrow S_1$ transition between unsubstituted oligofluorenes and **1a**−**e**.[27,35]

of the oligofluorene chromophores are red-shifted compared to the values reported for unsubstituted oligomers of the same length. For the system bearing one fluorene unit **1a**, the $\pi-\pi^*$ absorption is centered at 327 nm (3.79 eV) while fluorene exhibits a maximum at 301 nm (4.11 eV).[32] For **1b** with three fluorene units, a $\pi-\pi^*$ absorption maximum is located at 362 nm (3.43 eV) while terfluorene shows an absorption peak centered at about 350 nm (3.54 eV).[27,33] As the length of the oligofluorene fragment is increased, the differences in energy for the $S_0 \rightarrow S_1$ transition of **1a**−**e** and the corresponding unsubstituted oligofluorenes are reduced. This behavior suggested relatively weak participation of the quinolinolate groups in the overall conjugation of the longer systems **1d** and **1e** (Table 1).

Intramolecular energy transfer from the oligofluorene fragments to Alq_2(acac) moieties was observed in the steady-state emission spectra of **1a**−**e** in solution. In the materials **1a**−**b** comprising one and three fluorene units, respectively, only the emission from the quinolinolate units (∼550 nm) was detected regardless of the excitation wavelength (Figure 3, left). Excitation of the coordination polymers **1c**−**e** ($n = 5-9$) at 340 nm (mostly $\pi-\pi^*$ oligofluorene) resulted in two emission components centered at 410 and 550 nm (3.02 and 2.25 eV). These features are consistent with $S_1 \rightarrow S_0$ transitions from oligofluorene fragments and aluminum quinolinolate moieties, respectively. As one could expect, the emission corresponding to the oligofluorene becomes more prominent with an increasing number of fluorene units. This is explained by increased probability of populating conformational states with reduced conjugation along the oligofluorene backbone due to rotation around fluorene−fluorene bonds.

The excitation spectra of **1a**−**e** monitored at 550 nm (Figure 3, right) fully resembled the UV−visible absorption spectra suggesting reasonably effective migration of singlet excitons from oligofluorene bridges to the Alq_2(acac) moieties. This premise was further supported by the major contribution of the Alq_3-type fluorescence in the emission spectra, despite the significant length of the ligands (19−85 Å) and their high fluorescence quantum yield ($\Phi_{Fl} = 0.9-1.0$).[34] It was reasoned that the energy transfer must compete very effectively with the fast radiative decay of oligofluorene ($\tau_{Fl} = 400-800$ ps),[35,36] presumably as a result of exciton delocalization between both fluorophores. This possibility was further investigated by femtosecond UV−visible transient absorption spectroscopy.

Ultrafast Energy Migration in 1a−**e.** To monitor the energy transfer process in **1a**−**e**, we studied the spectral and kinetic features of each chromophore upon selective excitation. Thus, two model systems, aluminum(III) tris(5-phenyl-8-quinolinolate) (**2**) and terfluorene end-capped with trimethylsilyl groups (**3**), were studied first (Figure 4A). Upon excitation of **2** at 475 nm (2.61 eV, $\pi-\pi^*$ of Alq_3), positive absorption centered approximately at 520 nm along with a second feature of lower intensity between 540−760 nm were observed (Figure 4C). After its initial rise, the intensity of this spectrum did not decay significantly within the time window of the experiment (1.6 ns). Given the relatively long lifetime of this species, the observed transient spectrum was attributed to a transition of the singlet state $S_1 \rightarrow S_n$. This was further confirmed by monitoring this spectrum by transient UV−visible spectroscopy in a nanosecond regime as well as by the photoluminescence decay kinetics ($\tau_{Fl} = 9.72$ ns).[31]

Excitation of the oligofluorene model **3** at 340 nm (3.65 eV, $\pi-\pi^*$ of oligofluorene) resulted in broad absorption ranging between 475−760 nm after a quick initial rise (0.2 ps). Stimulated emission was also detected in the region of 400−475 nm as a negative signal (Figure 4D). The decay of this transient at 750 nm showed a monoexponential behavior with lifetime ($\tau = 642 \pm 4$ ps), which agreed with the reported fluorescence lifetimes for terfluorene obtained from up-conversion fluorescence studies.[36] Furthermore, the observed spectral features are in excellent agreement with literature reports of the absorption of singlet excited-state of oligofluorene,[37] which confirmed the nature of the oligofluorene excited state.

The considerable overlap between the spectral features of aluminum quinolinolate and oligofluorene required careful comparison of the transient spectra obtained for systems **1a**−**e**. Excitation of the coordination polymers **1a**−**e** under the same conditions employed for **2** ($\lambda_{exc} = 475$ nm, 1.5 mW) afforded the transient spectra displayed in Figure 5 (0.2 ps after a rise). The kinetics of these transients followed the behavior observed for the model **2**, thus confirming the selective formation of the singlet excited-state in the Alq_3-type moieties. Beside the absorption at 520 nm, a new band ($\lambda_{max} = 575-640$ nm) was observed in the spectra of **1a**−**e**. This band shifted toward lower energies and increased in intensity with a higher number of fluorene units, suggesting that quinolinolate−oligofluorene conjugation affected the spectrum of the excited state. Interestingly, the absorption maximum in **1c**−**e** with 5, 7, and 9 fluorene units, respectively, did not show a significant red shift compared to **1b** with only three fluorene units. This leveling off in the red-shift of the fluorene transient maxima suggests that regardless of the oligomer length the effect of conjugation is not significantly extended beyond three units.

Upon excitation of the oligofluorene moiety in **1a**−**e** under the same conditions employed for the terfluorene model system **3** ($\lambda_{exc} = 340$ nm, 0.5 mW), distinct transient spectra are observed (Figure 5, right). The shape of the spectra differed

(31) Montes, V. A; Pohl, R.; Shinar, J.; Anzenbacher, P., Jr. *Chem.−Eur. J.* **2006**, *12*, 4523.
(32) Montalti, M.; Credi, A.; Prodi, L.; Gandolfi, M. T. *Handbook of Photochemistry*; Taylor and Francis: Boca Raton, FL, 2006.
(33) Klaerner, G.; Miller, R. D. *Macromolecules* **1998**, *31*, 2007.
(34) Wong, K.-T.; Chien, Y.-Y.; Chen, R.-T.; Wang, C.-F.; Lin, Y.-T.; Chiang,.; Hsieh, P.-Y.; Wu, C.-C.; Chou, C. H.; Su, Y. O.; Lee, G.-H.; Peng, S.-M. *J. Am. Chem. Soc.* **2002**, *124*, 11576.
(35) (a) Chi, C.; Im, C.; Wegner, G. *J. Chem. Phys.* **2006**, *124*, 024907. (b) Lupton, J. M.; Craig, M. R.; Meijer, E. W. *App. Phys. Lett.* **2002**, *80*, 4489.
(36) (a) Wasserberg, D.; Dudek, S. P.; Meskers, S. C. J.; Janssen, R. A. J. *Chem. Phys. Lett.* **2005**, *411*, 273. (b) Anémian, R.; Mulatier, J.-C.; Andraud, C.; Stéphan, O.; Vial, J.-C. *Chem. Commun.* **2002**, 1608.
(37) (a) Cerullo, G.; Stagira, S.; Zavelani-Rossi, M.; De Silvestri, S.; Virgili, T.; Lidzey, D. G.; Bradley, D. D. C. *Chem. Phys. Lett.* **2001**, *335*, 27. (b) Cabanillas-Gonzalez, J.; Antognazza, M. R.; Virgili, T.; Lanzani, G.; Gadermaier, C.; Sonntag, M.; Strohgiel, P. *Phys. Rev. B.* **2005**, *71*, 155207.

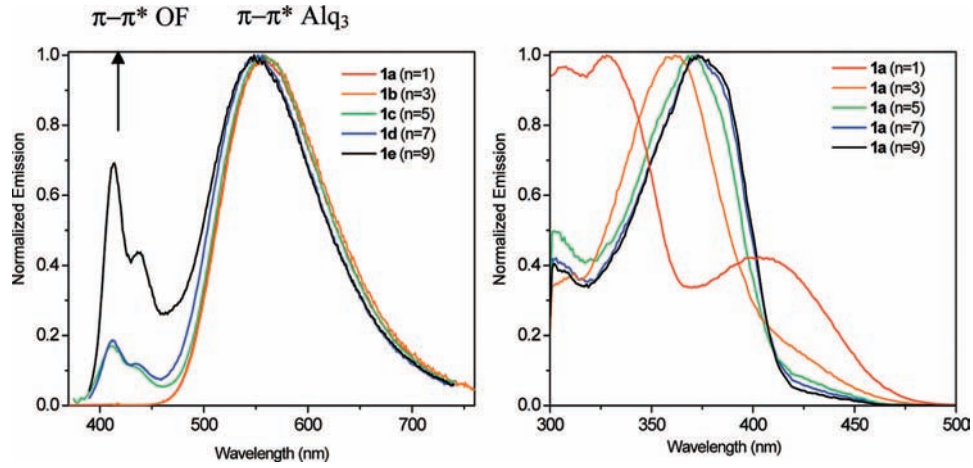

Figure 3. Left: Corrected emission spectra of the coordination polymers **1a**−**e** in CH_2Cl_2 upon excitation at 340 nm. Right: Excitation spectra of the polymers when monitored at 550 nm.

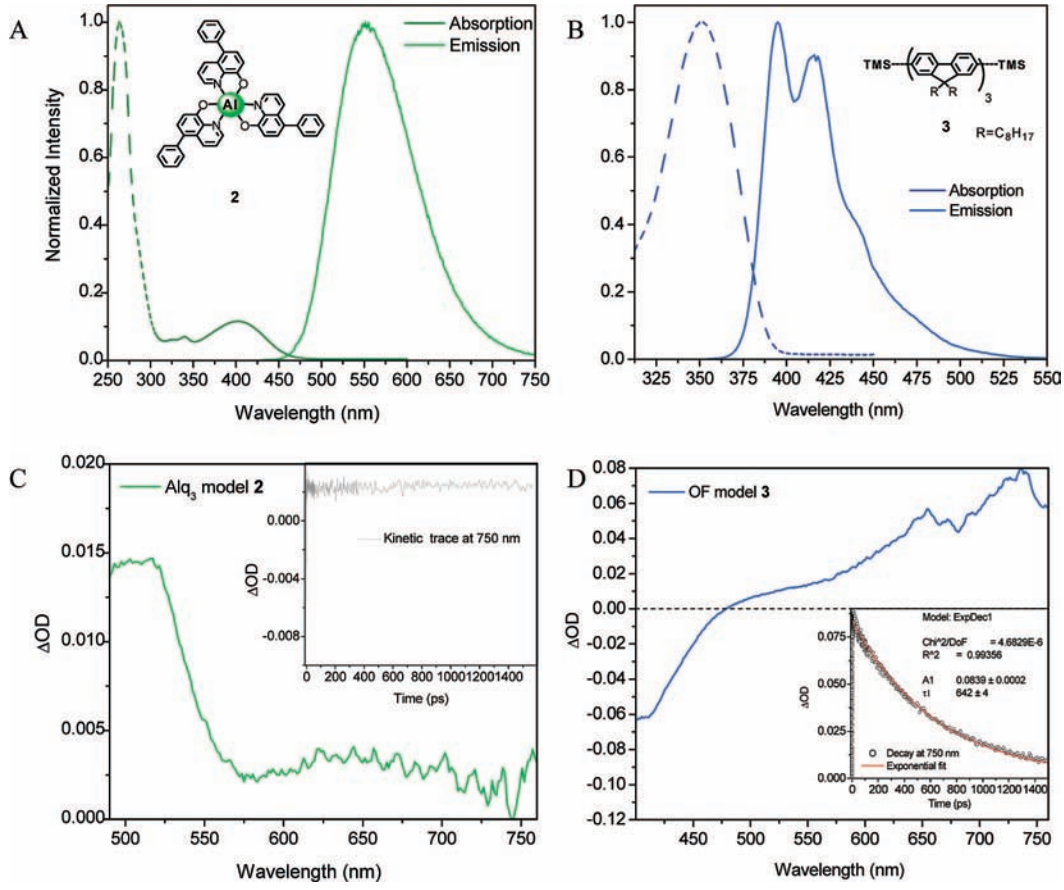

Figure 4. (A) Absorption and emission spectra of model compound **2**. (B) Absorption and emission spectra of model compound **3**. (C) Transient absorption spectra of **2** 0.2 ps after pump pulse at 475 nm and its decay monitored at 750 nm (inset). (D) Transient absorption spectra of **3** 0.2 ps after pump pulse at 340 nm and its decay monitored at 750 nm (inset).

dramatically in the series **1a**−**e** depending on the length of the oligofluorene segment. For systems **1a**−**b** ($n = 1, 3$) the spectra were essentially identical to transients observed upon excitation at 475 nm, suggesting a strong electronic coupling. The high degree of coupling observed for **1a**−**e** is consistent with the excited-state being distributed all over the two chromophores.[38] Transient spectra of **1c**−**e** ($n = 5-9$) comprised features attributable to both Alq_3 and the oligofluorene. Flattening of the band centered at 640 nm, a shift of the maximum of absorption to higher wavelengths, and the stimulated emission from oligofluorene were detected at early times ($\tau < 10$ ps) and were replaced by the features observed upon excitation at 475 nm (Figure 6). After the spectral evolution, the decay of the transients of **1a**−**e** also exhibited a long-lived state ($\tau \geq 1.6$ ns) attributed to the Alq_3-type singlet excited state. In summary, the observed transient spectra support the hypothesis

(38) Tinnefeld, P.; Heilemann, M.; Sauer, M. *ChemPhysChem* **2005**, *6*, 217.

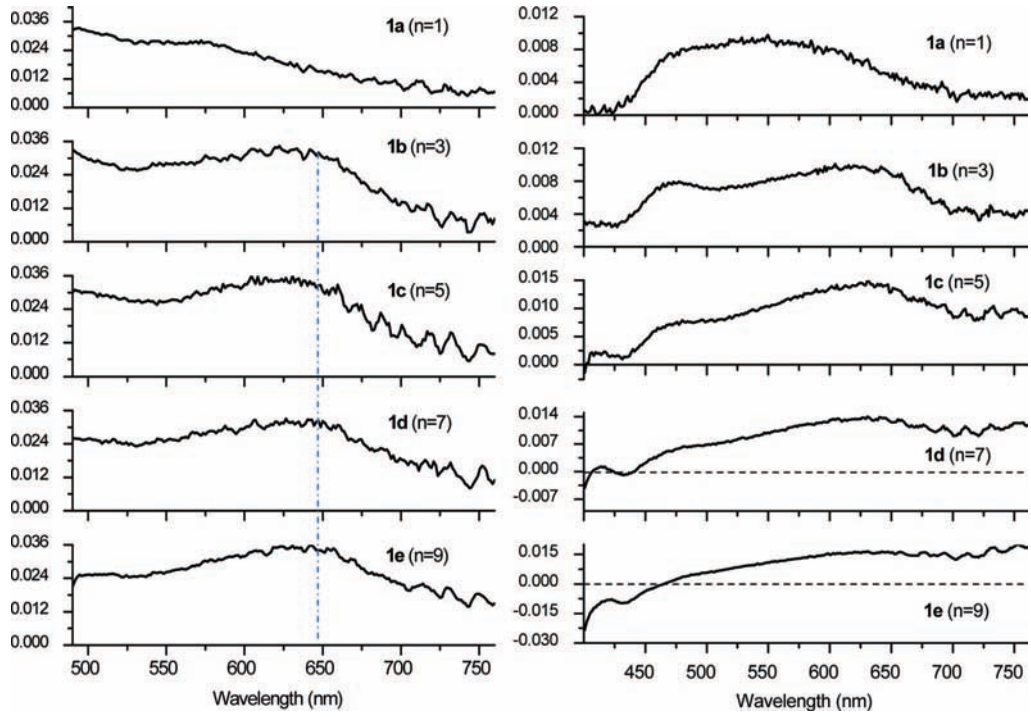

Figure 5. Left: Transient absorption spectra of **1a**−**e** 0.2 ps after excitation at 475 nm (1.5 mW). The dotted line indicates the saturation of the peak absorption around 640 nm. Right: Transient absorption spectra of **1a**−**e** 0.2 ps after excitation at 340 nm (0.5 mW).

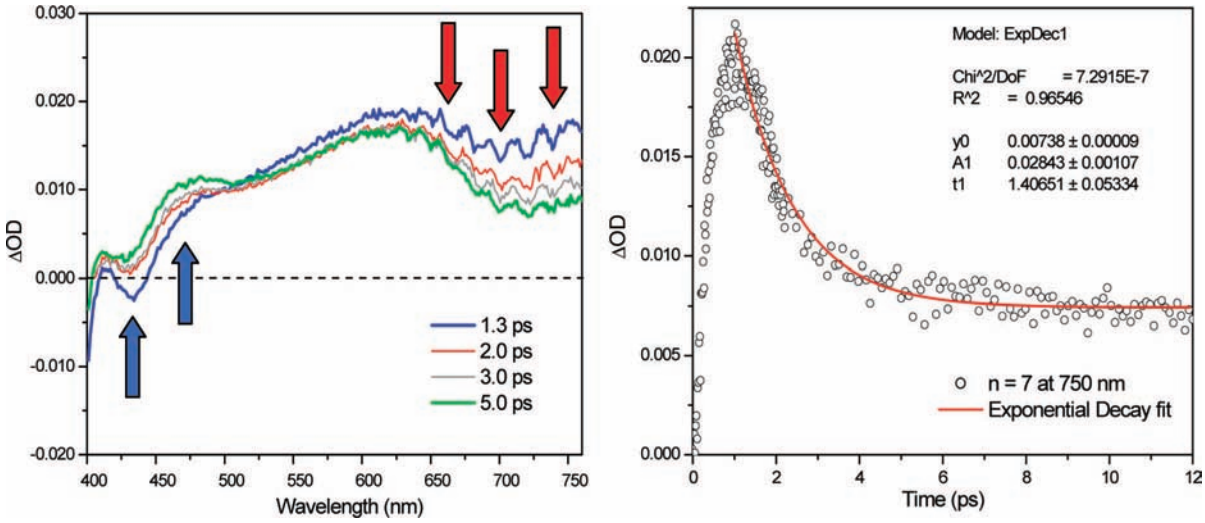

Figure 6. Left: Transient absorption spectra for **1d** after excitation at 340 nm (0.5 mW) at various times. Right: Exponential fit of the kinetic profile at 750 nm.

of efficient singlet energy transfer from oligofluorene to aluminum quinolinolate in these bichromophoric systems.

The observed spectral evolution allowed for assessment of the rate constant of the energy transfer process (Figure 6, right). Because of the significant change in intensity at 750 nm, this wavelength was selected for monitoring the kinetics of the energy transfer in **1c**−**e** (see Appendix, Supporting Information for additional spectra). The rate constant of the energy transfer from oligofluorene to aluminum quinolinolate was calculated using the equation:[39] $k_{ET} = \tau_{Obs}^{-1} - \tau_{Fl}^{-1}$, where k_{ET} is the overall rate of energy transfer, τ_{Obs} is the lifetime observed for the spectral change in the transient experiment, and τ_{Fl} represents the fluorescence lifetime of the energy donor in the absence of the acceptor. In all three cases, very short lifetimes corresponding to ultrafast energy transfer rate constants were obtained. A summary of the calculated values for the energy transfer rates is presented in Table 2. In all cases the estimated efficiency of energy transfer is above 99%,[40] which is in agreement with the

Table 2. Calculated Rate Constants for Energy Transfer in the Coordination Polymers **1c**−**e** Monitored by Decay at 750 nm

system	*n* (fluorene units)	τ_{Obs} (ps)	τ_{Fl} (ps)[a]	k_{ET} (s^{-1}) × 10^{11}
1c	5	1.45 ± 0.05	549	6.9 ± 0.2
1d	7	1.40 ± 0.05	505	7.1 ± 0.2
1e	9	2.99 ± 0.08	476	3.3 ± 0.1

[a] The lifetime values were adapted from the literature.[35a]

(39) Welter, S.; Lafolet, F.; Cecchetto, E.; Vergeer, F.; De Cola, L. *ChemPhysChem* **2005**, *6*, 2417.

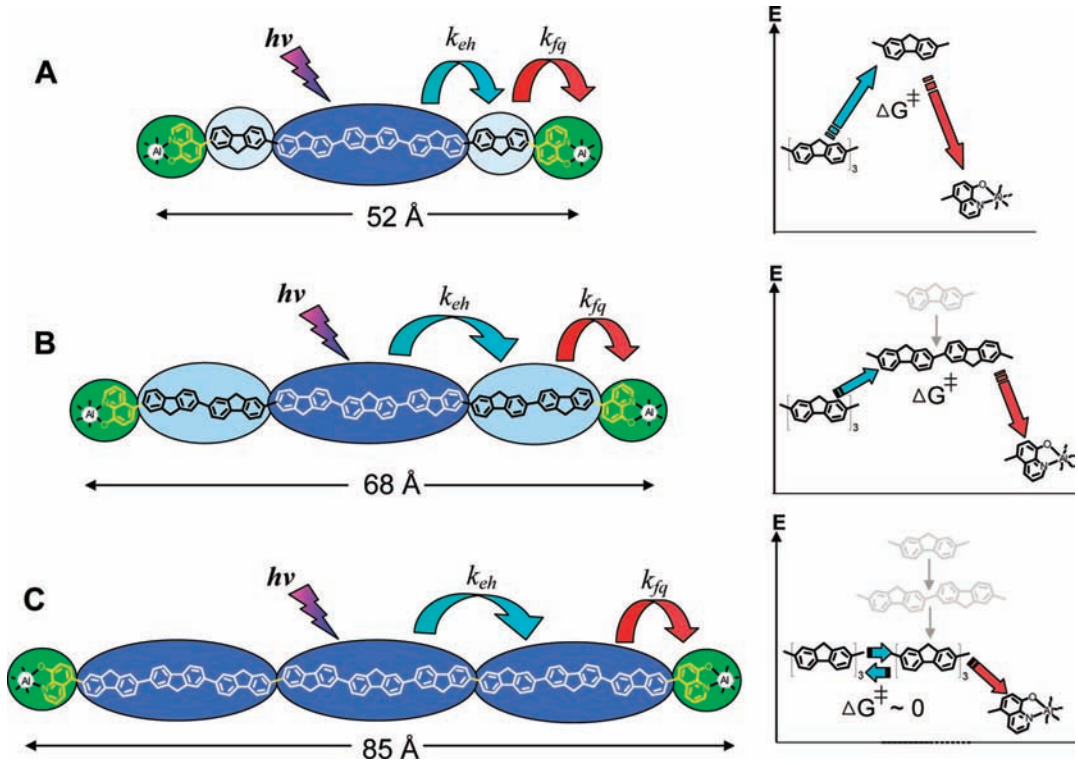

Figure 7. Schematic representation of the mechanism for intramolecular energy transfer as proposed for the behavior of the bichromophoric systems **1c**−**e**. Only one pathway of energy migration is shown for simplicity purposes.

results recorded in the steady state experiments (≥98%, see Supporting Information for details).

Comparison of the Experimental Results with the Improved Förster Theoretical Model. The exciton dynamics observed for systems **1a**−**e** were found to be in excellent agreement with the improved Förster formalism reported for description of energy transfer in this type of conjugated systems.[14b] According to the model, when a conjugated oligomer acts as an energy donor, the intramolecular energy transfer process consists of multistep exciton migration along the chain. This mechanism results in virtual shortening of the distance between the donor and acceptor, as well as a corresponding increase of the ultrafast energy transfer rates. The results from both steady-state photoluminescence and time-resolved absorption spectroscopy experiments confirm that the light absorption by the oligofluorene fragments in **1a**−**e** is followed by an ultrafast exciton migration ($k_{ET} = 3.3-7.1 \times 10^{11}$ s^{-1}) toward aluminum quinolinolate moieties of lower energy (Figure 7).

In general, the energy transfer rates in wirelike conjugated species are governed by the actual donor−acceptor spectral overlap and HOMO−LUMO levels, as well as the donor−acceptor electronic coupling, which depends on their actual distance. Figure 7 shows three examples of materials **1c**−**e** that differ in the three features above. Interestingly, the overall energy transfer rates (k_{ET}) found experimentally (Table 2) are $6.9 \pm 0.2 \times 10^{11}$, $7.1 \pm 0.2 \times 10^{11}$, and $3.3 \pm 0.1 \times 10^{11}$ s^{-1} for D−A distances of 52, 68, and 85 Å, respectively. Here, the k_{ET} is composed of two components corresponding to the exciton hopping between the fluorene moieties (k_{eh}) and the one corresponding to the strongly exothermic transfer from fluorene to Al^{III} quinolinolate (k_{fq}). While the fluorene-to-quinolinolate transfer is always exothermic and fast, the exciton hopping between the fluorene displays more complex energetics (Figure 7) and is likely to be a decisive factor to influence the final k_{ET}.

The fact that the initial increase of 16 Å in the D−A distance between **1c** and **1d** is accompanied by an actual increase in energy transfer rate is rationalized in terms of the model put forward by Beljonne et al.,[14b] which suggests that maximum rates for exciton hopping are observed for shorter donor and acceptor fragments (2−3 indenofluorene moieties corresponding to ca. three fluorene units). When the donor and acceptor size increases beyond those of "optimal conjugation lengths", the rates for exciton hopping decrease making the overall energy transfer process less efficient (i.e., k_{ET} is decreased). This assertion is based on the fact that the energy transfer requires both the spectral overlap of the decoupled donor/acceptor fragments as well as some degree of electronic coupling between them. In the material **1c** with five fluorene units (Figure 7A), the optimal donor (central terfluorene) is flanked by two single fluorene units. While the emission of the terfluorene donor is 390−450 nm, the absorption of single fluorene is in the deep UV. Thus, the forward exciton hopping (k_{eh}) is disfavored by an insufficient orbital overlap. The corresponding energy diagram shows the same feature in terms of the energies of the respective singlet excited states and the activation energy required for exciton hopping, which renders the energy transfer in **1c** less efficient. Needless to say, this particular distribution of fluorene moieties in **1c** shown in Figure 7A is not the only one possible but is the one most likely responsible for the relatively lower rate ($k_{ET} = 6.9 \pm 0.2 \times 10^{11}$ s^{-1}) in energy transfer in **1c** according to the model.[14b]

In the "intermediate" material **1d**, the terfluorene donor with "optimal conjugation length" is flanked with two acceptor moieties composed of two fluorene moieties that display a sufficient spectral overlap and require only moderate activation energy for forward exciton hopping (k_{eh}) from the donor to the

(40) $E = k_{ET}/(k_{ET} + \tau_F^{-1})$.

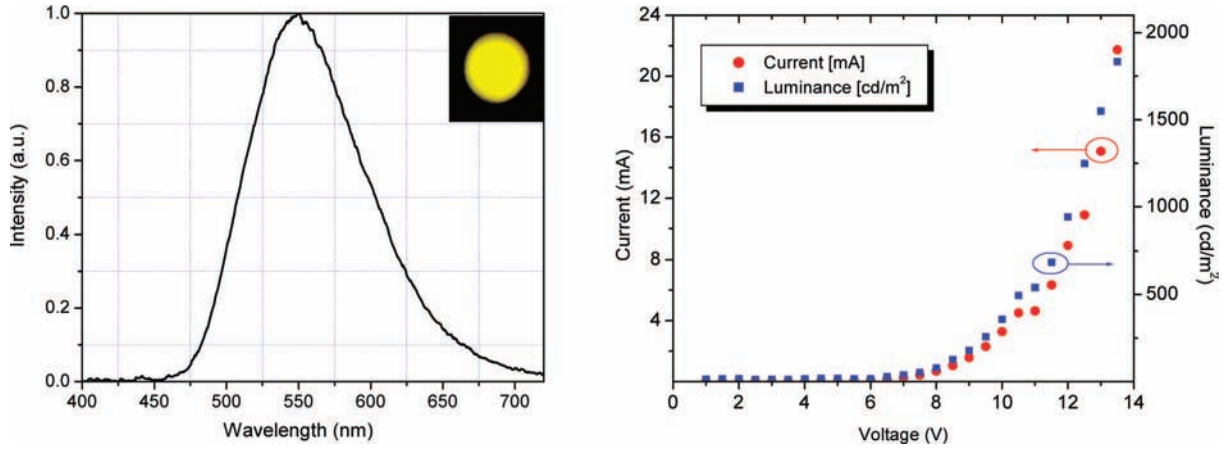

Figure 8. Left: Electroluminescence spectra of **1a**-OLED at a voltage of 9 V. The inset shows a photograph of the operating device. Right: $I-V$ and luminance curves of the ITO/PEDOT:PSS/**1a** /CsF:Al OLED. Turn-on voltage was ca. 6 V.

acceptor (Figure 7B). The combination of a shorter overall distance and moderate activation energy results in the highest overall rate ($k_{ET} = 7.1 \pm 0.2 \times 10^{11}$ s^{-1}) of the energy transfer in **1d**.

In the material **1e** displaying the D−A distance of roughly 42 Å (85 Å/2), the increasing size of the oligomer fragment results in smaller electronic coupling factors and reduced rates of energy transfer. Even though an almost isoenergetic pair may exist for the exciton migration in the oligofluorene backbone due to the better spectral overlap (Figure 7C), the exciton hopping simply competes less efficiently with radiative decay of the donor (k_{ET} decreases exponentially with the D−A distance in electronically coupled D−A pairs). As a result, **1e** displays the lowest energy transfer rate constant ($k_{ET} = 3.3 \pm 0.1 \times 10^{11}$ s^{-1}).

Solid-State Optical Properties and Electroluminescence. The solid-state emission of coordination polymers **1a**−**e** was evaluated by steady-state photoluminescence of their spin-coated thin films. For all materials only one type of emission (Alq_3-like) was detected regardless of the wavelength of excitation (see Supporting Information). The changes observed in the solid-state emission spectra of **1a**−**e** could be attributed to the interchain energy transfer pathways due to a close contact between the polymer chains[41] rather than to the increased degree of conjugation as a result of surface templating. It has been demonstrated that interchain energy migration can be more effective than intrachain energy transfer, which is limited by coupling of the excitations along the chain direction.[14a,b] In fact, more efficient energy transfer processes in the solid state have been reported to take place compared to diluted solutions for a wide range of covalently linked donor−acceptor systems comprising polyfluorenes.[42,43] Therefore, the disappearance of the oligofluorene emission component observed in solution for bichromophoric systems **1c**−**e** was attributed to efficient interchain energy transfer processes in the solid state. This was further confirmed by dispersing the polymers **1a**−**e** in an inert matrix (1% in PMMA) to minimize encounter of the emissive polymer chains in the film. Thin films of the dispersed polymers **1c**−**e** again exhibited both the fluorene-type and Al^{III}-quinolinolate fluorescence components indicating that the interchain energy transfer mechanism was suppressed by reducing the concentration of the polymer in the matrix (see Supporting Information).

Preliminary incorporation of the coordination polymers into OLEDs was performed by processing the materials by spin-coating. Simplified OLED architectures ITO/PEDOT:PSS(500 Å)/**1a**−**c**(600 Å)/CsF(10 Å):Al(1200 Å) were fabricated in order to confirm the electroluminescent abilities of these hybrid materials. Devices based on **1a**−**c** ($n = 1-3$) exhibited somewhat similar performance, suggesting the ability of these materials to transport both electrons and holes in an efficient manner. Overall, the maximum luminance was 6000 cd/m^2 with a turn-on voltage of ~6 V and a maximum external quantum efficiency of 0.4%. An improved quantum efficiency and higher luminance was obtained when a bathocuproin (BCP) hole-blocking layer was vapor-deposited on top of the emissive polymer. The resulting device displayed saturated yellow emission (CIE coordinates $X, Y = 0.440, 525$; Figure 8) and external quantum efficiency of 1.2%. On the basis of the comparison with the previously published data[44] describing metallopolymer OLEDs based on phosphorescent metallocomplexes, these results from the simple unoptimized fluorescence-only devices are encouraging. This is particularly true if one considers that due to the quantum statistics of electron−hole recombination, the fluorescence-only devices are believed to have an upper theoretical efficiency limit of ca. 25% due to the statistical probability of obtaining one singlet exciton per three nonradiatively decaying triplet excitons.[45]

Conclusions

Novel coordination polymers comprising oligofluorene moieties of a varying size ($n = 1-9$) connected via aluminum(III) bis(8-quinolinolate)acetylacetone (Alq_2(acac)) complexes were synthesized and their photophysical properties were studied. Due to the bichromophoric nature of the polymers stemming from the oligofluorene and quinolinolate moieties, these materials display interesting photonic behavior. Thus, the singlet energy transfer in these coordination polymers was investigated by

(41) Cornil, J.; Beljonne, D.; Calbert, J.-P.; Brédas, J.-L. *Adv. Mater.* **2001**, *13*, 1053.
(42) Ling, Q. D.; Kang, E. T.; Neoh, K. G. *Macromolecules* **2003**, *36*, 6995.
(43) Huang, F.; Hou, L.; Wu, H.; Wang, X.; Shen, H.; Cao, W.; Yang, W.; Cao, Y. *J. Am. Chem. Soc.* **2004**, *126*, 9845.
(44) (a) Sandee, A. J.; Williams, C. K.; Evans, N. R.; Davies, J. E.; Boothby, C. E.; Kohler, A.; Friend, R. H.; Holmes, A. B. *J. Am. Chem. Soc.* **2004**, *126*, 7041. (b) Evans, N. R.; Devi, L. S.; Mak, C. S. K.; Watkins, S. E.; Pascu, S. I.; Köhler, A.; Friend, R. H.; Williams, C. K.; Holmes, A. B. *J. Am. Chem. Soc.* **2006**, *128*, 6647.

steady-state techniques and time-resolved absorption spectroscopy in the femtosecond regime. Strong electronic coupling between the chromophores is evidenced by the single spectral behavior of materials comprising shorter oligofluorene fragments **1a**−**b** ($n = 1, 3$). For materials **1c**−**e** with longer oligofluorene segments ($n = 5$, 7, and 9), spectral features from both quinolinolate and oligofluorene chromophores were observed. The energy migration from oligofluorene to the quinolinolate moieties was observed proceeding at a rate order of 10^{11} s^{-1}. The exact determination of energy transfer rates was possible by the well-defined discrete structure and purity of the building blocks, which could be purified to achieve high purity because of their small-molecule nature. The energy transfer behavior described for systems **1a**−**e** was rationalized according to the theoretical model proposed by Beljonne for the treatment of exciton migration in rigidly linked conjugated polymer systems. These results represent clear experimental evidence to support this model for intramolecular singlet−singlet energy transfer.

In the solid state, complete energy transfer from oligofluorene fragments to the quinolinolate centers was observed due to intermolecular energy transfer. Preliminary experiments with simple two- and three-layer devices fabricated by spin-coating yield bright yellow electroluminescence with maximum brightness of 6000 cd/m^2 with a turn-on voltage of ∼6 V, and a maximum external quantum efficiency of up to 1.2% suggesting their potential in PLED applications. These results may open up the possibility of controlling not only the emission color but also the semiconducting properties of novel materials by balancing charge transport through well-defined conjugated fragments.

Acknowledgment. Support from the NSF (Grant No. DMR-0306117 to P.A.), A. P. Sloan Foundation (P.A.), Air Force Office of Scientific Research (FA9550-05-1-0276), Ohio Laboratory for Kinetic Spectrometry, and McMaster Endowment for a McMaster fellowship to V.A.M. is acknowledged. We thank Professor Michael A. J. Rodgers for helpful discussions and Professor Anne J. McNeil for GPC analyses.

Supporting Information Available: General methods, synthesis and characterization of **1a**−**e**, X-ray crystallographic data (CIF file) of Alq_2acac, additional optical spectra, quantitative analysis of the steady-state PL, and fabrication of the OLEDs. This material is available free of charge via the Internet at http://pubs.acs.org.

JA805175W

(45) (a) Friend, R. H.; Gymer, R. W.; Holmes, A. B.; Burroughes, J. H.; Marks, R. N.; Taliani, C.; Bradley, D. D. C.; Dos Santos, D. A.; Brédas, J. L.; Löglund, M.; Salaneck, W. R. *Nature* **1999**, *397*, 121–128. Although the theory of 25% spin-degeneracy statistical limit has been recently subjected to modification, the fact remains that the efficiency of OLEDs is drastically limited by spin selection rules. (b) Shuai, Z.; Beljone, D.; Silbey, R. J.; Brédas, J. L. *Appl. Phys. Lett.* **2000**, *84*, 131–134. (c) Wohlgenannt, M.; Tandon, K.; Mazumdar, S.; Ramasesha, S.; Vardeny, Z. V. *Nature* **2001**, *409*, 494–496.